A NEW HYDRODYNAMIC MODEL USING AN EXACT RIEMANN SOLVER*

Zuzana Fecková[a,b], Boris Tomášik[b,c]

[a]University of Pavol Jozef Šafárik, Šrobárova 2, 04001 Košice, Slovakia
[b]Matej Bel University, Tajovského 40, 97401 Banská Bystrica, Slovakia
[c]FNSPE, Czech Technical University in Prague
Břehová 7, 11519 Prague 1, Czech Republic

(Received May 21, 2015)

Hydrodynamic modelling of quark–gluon plasma requires sophisticated numerical schemes that have low numerical viscosity and are able to cope with high gradients of energy density that may appear in initial conditions. We propose to use the Godunov method with an exact Riemann solver for ideal hydrodynamic modelling to meet these conditions. We present the results of numerical tests of the method, such as the sound wave propagation and the shock tube problem, which show both high precision of the method and low numerical viscosity.

DOI:10.5506/APhysPolBSupp.8.307
PACS numbers: 24.10.Nz

1. Introduction

Creation of the quark–gluon plasma and its expansion in heavy-ion collisions are phenomena widely studied both theoretically and experimentally. The hot and dense matter expands rapidly and it has been seen that the expansion can be very successfully modelled hydrodynamically [1, 2]. In the present paper, we will briefly introduce the equations of relativistic hydrodynamics. Then, we will explain the numerical scheme for hydrodynamic modelling of heavy-ion collisions which we have developed. We show results of various numerical tests and argue that the scheme is suitable for such modelling.

* Presented at "Excited QCD 2015", Tatranská Lomnica, Slovakia, March 8–14, 2015.

2. Hydrodynamic modelling

2.1. Relativistic hydrodynamics

Ideal relativistic hydrodynamic equations have the following form:

$$\partial_\mu n^\mu = 0\,, \tag{1}$$
$$\partial_\mu T^{\mu\nu}_{(0)} = 0\,, \tag{2}$$

where n^μ is the flow of a conserved charge. The relevant charge in nuclear collisions is usually the baryon number with the density n_B. Its flow is given as $n^\mu = n_B u^\mu$, where $u^\mu = \gamma(1, \vec{v})$ is the flow velocity and $\gamma = 1/\sqrt{1-v^2}$ is the Lorentz factor. Our model covers nuclear collisions at highest energies, where the net baryon density is practically zero. Therefore, we will not consider the first equation at all and solve only the second equation that expresses the conservation of energy and momentum. There, $T^{\mu\nu}_{(0)}$ is the energy and momentum tensor in non-dissipative case, with the explicit form

$$T^{\mu\nu}_{(0)} = (\epsilon + p)u^\mu u^\nu - p g^{\mu\nu}\,, \tag{3}$$

where ϵ is energy density, p is pressure and $g^{\mu\nu} = \mathrm{diag}(1,-1,-1,-1)$ is the Minkowski metric. Equation (2) can be rewritten in a different form, useful for numerical implementation, where we employ a vector of conserved variables U and spatial flow of the conserved variables $F(U)$

$$\partial_t U + \partial_x F(U) = 0\,, \tag{4}$$

where

$$U = \left((\epsilon+p)\gamma^2 - p, (\epsilon+p)\gamma^2 v^1, (\epsilon+p)\gamma^2 v^2, (\epsilon+p)\gamma^2 v^3\right)^T\,, \tag{5}$$
$$F^i = \left((\epsilon+p)\gamma^2 v^i, (\epsilon+p)\gamma^2 v^i v^1 + \delta^{i1}p,\right.$$
$$\left.(\epsilon+p)\gamma^2 v^i v^2 + \delta^{i2}p, (\epsilon+p)\gamma^2 v^i v^3 + \delta^{i3}p\right)^T\,. \tag{6}$$

2.2. Numerical scheme

Equation (4) is solved numerically by discretization of space into cells. We use the Godunov method with an exact Riemann solution at the interface. To obtain the value of conserved variables U, at the next time step, we solve a local Riemann problem at each boundary between neighbouring cells using linearly reconstructed variables in each cell. Its solution allows us to compute fluxes of conserved variables $F(U)$ at the interface [3, 4]. For a given cell, we then obtain the values of conserved variables at the next time-step by averaging the fluxes on the left and right boundary of the cell

$$U_i^{t+\Delta t} = U_i^t + \frac{\Delta x}{\Delta t}\left(F_{i+1/2} - F_{i-1/2}\right)\,, \tag{7}$$

where U_i^t is the value of a variable in the i^{th} cell at time t, and $F_{i-1/2}(F_{i+1/2})$ is the flux at its left (right) boundary.

3. Numerical tests

3.1. Sound wave propagation

For sound wave propagation test, we simulate a sound wave over one wavelength in the numerical grid by imposing the following initial conditions:

$$\begin{aligned} p_{\text{init}}(x) &= p_0 + \delta p \sin\frac{2\pi x}{\lambda}\,, \\ v_{\text{init}}(x) &= \frac{\delta p}{c_{\text{s}}(\epsilon_0 + p_0)} \sin\frac{2\pi x}{\lambda}\,, \end{aligned} \tag{8}$$

with parameters $p_0 = 10^3$ fm^{-4}, $\delta p = 10^{-1}$ fm^{-4}. Since the variation of pressure is sufficiently small $\delta p \ll p_0$, we can consider the linearized analytic solution, which is a sound wave of velocity c_{s}. The existence of the analytic solution allows us to evaluate the precision of our numerical scheme by comparing this solution to the values obtained by numerical computation. The precision is studied with $L1$ norm evaluated after one cycle, that corresponds to the period of the wave, with different numbers of cells in the numerical grid N_{cell} [5]

$$L\left(p\left(N_{\text{cell}}\right), p_s\right) = \sum_{i=1}^{N_{\text{cell}}} |p(x_i; N_{\text{cell}}) - p_s(x_i)| \frac{\lambda}{N_{\text{cell}}}\,. \tag{9}$$

The dependence of $L1$ norm on the number of cells is shown in the left panel of Fig. 1. The precision improves with finer discretization, as expected, and is similarly good as in other schemes presented in [5]. The numerical computation introduces dissipation into our solution even though we are solving ideal hydrodynamic equations. Since quark–gluon plasma is expected to have very low viscosity, we have to keep the artificial dissipation due to numerical scheme very low. We have evaluated the numerical viscosity of the scheme η_{num}, using the $L1$ norm

$$\eta_{\text{num}} = -\frac{3\lambda}{8\pi^2} c_{\text{s}}(\epsilon_0 + p_0) \ln\left[1 - \frac{\pi}{2\lambda\delta p} L(p(N_{\text{cell}}), p_s)\right]\,. \tag{10}$$

The dependence of numerical viscosity η_{num} on the number of cells in the grid is shown in the right panel of Fig. 1. Similarly to the dependence of $L1$ norm, it decreases with the number of cells and its values are adequately small. We have also estimated a more suitable parameter — the ratio of numerical viscosity and entropy density in our scheme η_{num}/s. We present

its values in Fig. 2 together with values of η/s for pion gas [6] and the limiting value of η/s for quark–gluon plasma from AdS/CFT calculations $1/4\pi$ [7].

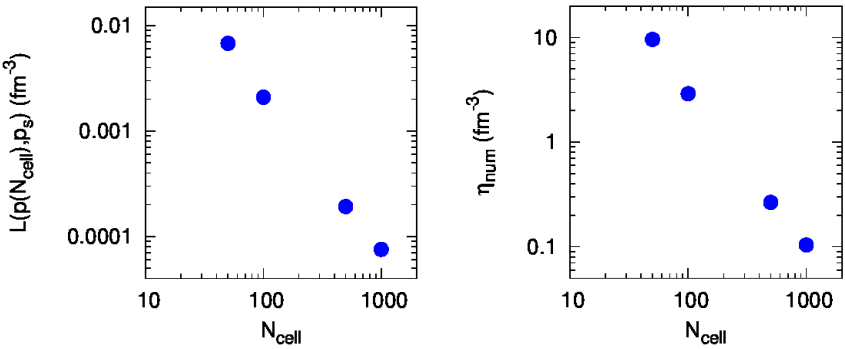

Fig. 1. Dependence of $L1$ norm (left) and numerical viscosity $\eta_{\rm num}$ (right) on number of cells in the numerical grid.

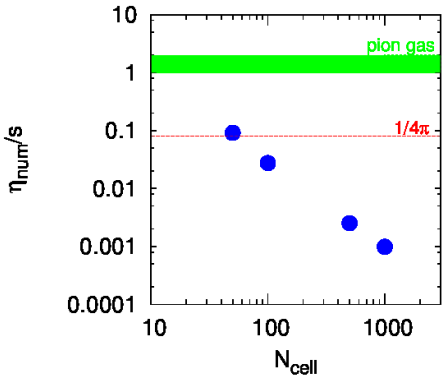

Fig. 2. Dependence of the numerical viscosity to entropy density ratio $\eta_{\rm num}/s$ (black/blue points) compared to the limiting value $\eta/s = 1/4\pi$ (thin/red line) and η/s of pion gas (grey/green band).

3.2. Shock tube problem

The shock tube problem is designed to test the capability of the scheme to cope with discontinuities in energy density. It consists of imposing special initial conditions in the numerical grid with two constant states separated by a discontinuity. The imposed energy density in the left (right) half is: $\epsilon_{\rm L} = 1$ GeV ($\epsilon_{\rm R} = 20$ GeV). The initial normal velocity is $v^x = 1/2c$ over the whole grid, the tangential velocity varies from the left to the right half: $v^{\rm t}_{\rm L} = 1/3c$, $v^{\rm t}_{\rm R} = 1/2c$. With time, we expect to see the dissolution of the discontinuity into a rarefaction wave propagating to the right, to the region

of higher energy density, and a shock wave propagating to the left, where energy density is lower. The shock tube problem has an analytic solution, which allows a good comparison between the numerical and exact solution.

In the left panel of Fig. 3, we show the profile of energy density in the grid after 100 time-steps. We see that the numerical solution (blue crosses) reproduces the analytic solution (black dashed line) accurately. The scheme is able to handle the initial discontinuity very well, which is also displayed in the right panel of Fig. 3 where the profile of normal velocity is shown after 100 time-steps. In Fig. 4, we compare the accuracy of the scheme

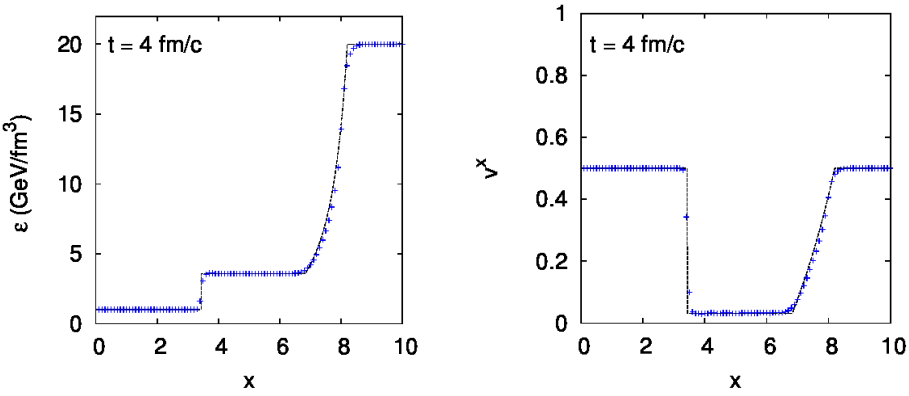

Fig. 3. Profile of energy density ϵ (left) and normal velocity v (right) in the numerical grid after 100 time-steps (our scheme — blue croses, analytic solution — black dashed line).

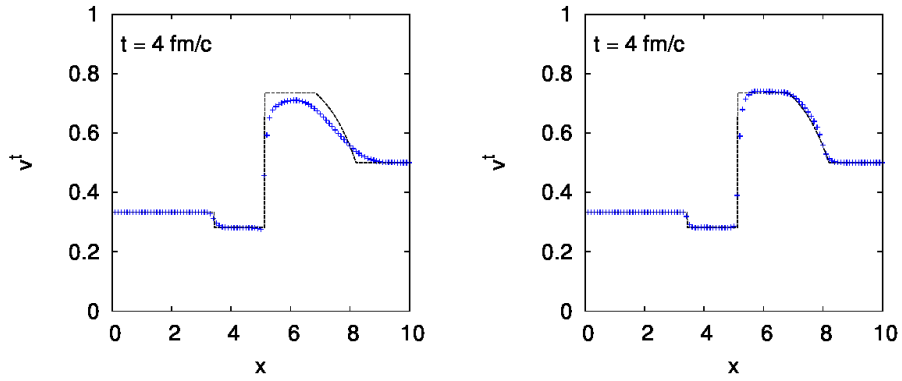

Fig. 4. Profile of tangential velocity v_{t} using a piecewise constant distribution of variables (left) and using a linear reconstruction of states (right) in the numerical grid after 100 time-steps (our scheme — blue crosses, analytic solution — black dashed line).

with and without the linear reconstruction of data. The difference is best seen in the profile of tangential velocity after 100 time-steps. The left panel of Fig. 4 shows this profile (numerical solution — blue crosses, analytic solution — black dashed line) with piecewise constant distribution of data, while the right panel shows the profile using the linear reconstruction, which clearly obtains better results, having only minor problems at the tail of the rarefaction wave.

4. Outlook

We have built and tested an ideal relativistic hydrodynamic scheme based on the exact solution of Riemann problem. The presented tests in one spatial dimension with presence of tangential velocity show a good resolution and ability to capture shock and rarefaction very well. We will extend this scheme to three dimensions and then apply it in a description of the flow in ultrarelativistic nuclear collisions.

This work has been partially supported by grant APVV-0050-11 (Slovakia). Z.F. also acknowledges support from VVGS-PF-2014-442 (Slovakia) and B.T. from MŠMT grant LG13031 (Czech Republic).

REFERENCES

[1] P. Romatschke, *Int. J. Mod. Phys. E* **19**, 1 (2010).
[2] C. Gale, S. Jeon, B. Schenke, *Int. J. Mod. Phys. A* **28**, 1340011 (2013).
[3] S.K. Godunov, *Mat. Sbornik* **47**, 357 (1959).
[4] J.A. Pons, *J. Fluid Mech.* **422**, 125 (2000).
[5] Y. Akamatsu *et al.*, *J. Comput. Phys.* **256**, 34 (2014).
[6] S. Mitra, S. Sarkar, *Phys. Rev. D* **87**, 094026 (2013).
[7] G. Policastro, D.T. Son, A.O. Starinets, *Phys. Rev. Lett.* **87**, 081601 (2001).